NATIONAL ADVISORY COMMITTEE
FOR AERONAUTICS

TECHNICAL NOTE

No. 1410

AN IMPROVED PHOTOELASTIC METHOD FOR DETERMINING

PLANE STRESSES

By C. B. Norris and A. W. Voss

Forest Products Laboratory

Washington

January 1948

NATIONAL ADVISORY COMMITTEE FOR AERONAUTICS

TECHNICAL NOTE NO. 1410

AN IMPROVED PHOTOELASTIC METHOD FOR DETERMINING PLANE STRESSES

By C. B. Norris and A. W. Voss

SUMMARY

An improved photoelastic method has been developed for determining stress concentrations which occur in nonisotropic materials under load. Drucker's method has been extended by means of an additional oblique photograph, and simpler equations for relating fringe order to principal stresses were obtained. The present method is considered more accurate than Drucker's and also provides a means of determining the directions of the principal stresses. The determination of these directions, how- ever, is not sufficiently accurate, and the use of a stress coat was found desirable for greater accuracy.

INTRODUCTION

One of the pertinent problems involved in the use of nonmetallic materials for aircraft construction is the determination of the stress concentrations which occur in such nonisotropic materials under load. In an investigation of this problem the first type of stress distribu- tion selected for study was that which occurs around a loaded bolt passing through nonisotropic materials. In order to attack this problem, a photoelastic method has been developed. The present report describes this method and also its use in determining stress distributions in a loaded bolt. A review of the literature at the outset of the investi- gation indicated that the existing methods of photoelastic stress analysis were not entirely suitable for use in the problem under study. The usual and more simple photoelastic methods require the model to have a free edge, a requirement difficult to fulfill in this case.

In order to overcome this limitation, several methods for analysis at single points have been developed (references 1 and 2), but these become tedious when analysis over an area is attempted. Others (references 3 and 4) that are more suitable for analysis over an area require special apparatus as well as extreme care in the preparation of models.

Drucker's oblique-incidence method (reference 5) is essentially a point-by-point procedure unless his more complicated general equations

can be made applicable. Frocht states their use is practicable (reference 6), but according to Drucker they cannot be applied accurately.

It was found in the present study that Drucker's method can be extended and made more useful by means of an additional oblique photograph and that simpler equations for relating fringe order to principal stresses can be obtained. The resulting procedure developed in the present investigation is considered more accurate than Drucker's original one, and, in addition, makes available a means of determining the directions of the principal stresses. The determination of these directions, however, is not sufficiently accurate, and the use of a stress coat (reference 7) was found desirable for greater accuracy.

This work was conducted at the Forest Products Laboratory under the sponsorship and with the financial assistance of the National Advisory Committee for Aeronautics.

APPARATUS

An apparatus was designed and built to utilize the double-oblique method of photoelastic analysis. The light, lenses, and camera for the polariscope were mounted on a track supported by a frame and bars (fig. 1). Each of the two side members of the frame was mounted on crossed pins that permitted the light to come from any direction within 0° to 45° of the normal position.

The polariscope and supporting rig in position in a testing machine are shown in figure 1. The essential parts of the polariscope from left to right are transformer; mercury vapor lamp, filter, and 10-inch lens, the last three items covered by the shield; $8\frac{1}{4}$- inch-diameter polarizing plate; quarter-wave plate; space for the specimen; quarter-wave plate; analyzing plate; 10-inch lens; and camera with 8- by 10-inch ground-glass viewing plate. These items are mounted on tracks that are pin-connected to the cross bars. The cross bars are free to pivot on the bolt hangers. A graduated quadrant mounted on the left end of the second cross bar is read against a pointer attached to the bolt hanger to determine the angle between the line through the horizontal pivots and the optic axis. The bolt hangers are suspended from channel iron members. Each channel is supported by a pin parallel to the hangers, and these pins are supported by alined horizontal pins. The angle between the horizontal plane and the projection of the optic axis on a plane perpendicular to the horizontally alined pins is read by means of a graduated quadrant mounted on the base and a pointer mounted on the horizontal pin. The supporting structure is made of pipe, channels, and bars welded together to leave access to the base of the testing machine and to the space for the specimen. Counterweights are placed where necessary to balance the assembly about the crossed pivots.

THEORY OF IMPROVED PHOTOELASTIC METHOD

Drucker's general equations are:

$$n_p = \frac{-n_n(1 + \cos^2 \phi)\cos 2\theta \pm 2\cos\phi\left(n_o{}^2 - n_n{}^2\sin^2 2\theta\right)^{1/2}}{2\sin^2 \phi} + \frac{n_n}{2} \quad (1)$$

$$n_q = \frac{-n_n(1 + \cos^2 \phi)\cos 2\theta \pm 2\cos\phi\left(n_o{}^2 - n_n{}^2\sin^2 2\theta\right)^{1/2}}{2\sin^2 \phi} - \frac{n_n}{2} \quad (2)$$

where the symbols are defined as follows:

n_p fringe order for the algebraically larger of the principal stresses p

n_q fringe order for the other principal stress q

n_n fringe order from photograph with light normal to surface of model

n_o fringe order from photograph with light oblique to surface of model

ϕ angle between direction of light inside model and a normal to its surfaces

θ orientation of p measured counterclockwise from x-axis

Let $n_x = n_p + n_q$; then, adding equations (1) and (2) gives

$$n_x = \frac{-n_n(1 + \cos^2 \phi)\cos 2\theta \pm 2\cos\phi\left(n_o{}^2 - n_n{}^2\sin^2 2\theta\right)^{1/2}}{\sin^2 \phi} \quad (3)$$

This equation may be put in the form:

$$n_x{}^2 \sin^4 \phi + 2n_x n_n(1 + \cos^2 \phi)\sin^2 \phi \cos 2\theta + n_n{}^2 \sin^4 \phi \cos^2 2\theta$$

$$+ 4\left(n_n{}^2 - n_1{}^2\right)\cos^2 \phi = 0 \quad (4)$$

where n_1 is the fringe number in the oblique photograph.

An additional oblique photograph is taken with the light beam rotated so that the plane defined by its axis and the normal is at angle of 90°

to the similar plane associated with the first oblique photograph. Equation (4) applies also to this photograph if θ is replaced by $\theta + \frac{\pi}{2}$; that is, the value of $\cos 2\theta$ is reversed in sign. On inserting n_2, the fringe number from the second oblique photograph, in place of n_1 and changing the sign of $\cos 2\theta$, equation (4) becomes

$$n_x{}^2 \sin^4 \phi - 2n_x n_n (1 + \cos^2 \phi) \sin^2 \phi \cos 2\theta + n_n{}^2 \sin^4 \phi \cos^2 2\theta$$

$$+ 4\left(n_n{}^2 - n_2{}^2\right) \cos^2 \phi = 0 \qquad (5)$$

Subtracting equation (5) from equation (4) leaves

$$4n_x n_n (1 + \cos^2 \phi) \sin^2 \phi \cos 2\theta + 4\left(n_2{}^2 - n_1{}^2\right) \cos^2 \phi = 0 \qquad (6)$$

which can be put in the form:

$$\frac{n_x}{n_n} = \frac{n_1{}^2 - n_2{}^2}{n_n{}^2} \frac{\cos^2 \phi}{(1 + \cos^2 \phi) \sin^2 \phi \cos 2\theta} \qquad (7)$$

The values of n_1, n_2, and n_n at any point in an area may be determined from one group of photographs. The angle ϕ is the angle between the oblique ray of light inside the model and a normal to the surfaces of the model. The angle θ is measured by using the stress-coat technique. The value of n_x is determined by using these values in equation (7). It may be noted that no serious confusion of sign results from the use of this equation. The principal stresses are then easily determined:

$$\left.\begin{array}{l} n_x = n_p + n_q \\ \\ n_n = n_p - n_q \end{array}\right\} \qquad (8)$$

Addition gives twice the fringe number for one principal stress, and subtraction gives twice the fringe number for the other. Equation (7) becomes indeterminate when $\theta = \frac{\pi}{4}$ and $n_1 = n_2$, but this difficulty

may be avoided by taking an additional pair of oblique photographs at an angle of 45° to the first pair.

Equations (7) and (8) have the following advantages over equations (3) to (6) of Drucker's paper (reference 5):

1. Equation (7) is general; it applies for any position of the principal axes of stress.

2. Drucker defines n_p as algebraically larger than n_q. This leaves some doubt regarding the identification of n_p and n_q. Equations (7) and (8) make this identification clear.

3. The right-hand member of equation (7) is independent of the sign of n_n, n_1, and n_2; thus the ratio n_x/n_n has a unique value. This eliminates the confusion in the use of Drucker's equations because the sign of n_0 is not known.

4. Both methods are concerned with differences of fringe values measured from two photographs. The differences encountered by Drucker are $n_0 - n_n \cos \theta$ and $n_0 \cos \theta - n_n$ (in Drucker's notation). The differences encountered in the method described herein are $n_1^2 - n_2^2$ or $\left(n_1 + n_2\right)\left(n_1 - n_2\right)$. Usually the value of $n_1 - n_2$ is about double that of $n_0 - n_n$, and the accuracy of the present method is therefore about twice that of Drucker's.

COMPARISON OF RESULTS FROM PHOTOELASTIC METHOD AND ELASTIC THEORY

A 2-inch-diameter circular disk 0.252 inch thick was loaded in compression at opposite ends of a diameter. This model was placed so that its central plane was vertical and contained the line between the horizontal pivots of the polariscope jig. Before load was applied, two photographs were taken with the light normal; one photograph is shown in figure 2 with white background and one in figure 3 with dark background to show the initial fringe pattern. Load was then applied through round steel rods 0.125 inch in diameter. Photographs were taken with both white and dark backgrounds and with light direction (1) normal, (2) rotated vertically 45°, (3) rotated horizontally 45°, and (4) rotated 48° 19' from the normal in a 45° plane. These are shown respectively in figures 4 to 11. The photographs shown in figures 10 and 11 were taken to provide data near the ends of the diagonal diameter of the model because of the possibility that data from the other photographs might lead to indeterminate values of equation (7). This difficulty

was not encountered in the analysis, and therefore the data from these
photographs were not employed. After the fringe patterns under load
had been photographed, the load was removed and the photograph in
figure 12 was taken to show the residual fringe pattern in the vicinity
of the concentrated loads.

The model was later sprayed with a stress-indicating lacquer. After
the lacquer dried, load was again applied. Cracks perpendicular to the
principal tensile stress formed in the lacquer. These were dye-etched
to preserve them. After the coated specimen had remained under load
about 1 hour, the lacquer and the model were chilled with air passed over
dry ice. The load was immediately released; the result was a formation
of cracks perpendicular to the principal compressive stress. These also
were dye-etched. A photograph of the etched cracks is shown in figure 13.

A circle 1.20 inches in diameter had been drawn on each surface of
the disk so that correct measurements could be made on the prints in
units of the radius of the scribed circle. A transparent interpolator
was used to read the location of fringes to a radius of 0.01. Curves
with fringe number as ordinate and distance from the center of the model
as abscissa were prepared for the vertical diameter of the disk (fig. 14),
the horizontal diameter (fig. 15), and a diameter at 45° to the vertical
diameter (fig. 16). The values of the angle θ between direction of
principal stress at various points along a 45° diameter and the x-axis
were determined from the photograph in figure 13 and are plotted in
figure 17. The index of refraction was obtained from the rotated views
showing the two scribed circles displaced in the horizontal and in the
vertical directions.

From the values of n_1, n_2, n_n, θ, and ϕ so obtained, the
values of n_x were computed (by equation (7)) for several points on
the vertical, horizontal, and 45° diameters. From n_x and n_n, the
values of n_p and n_q were obtained and are plotted in figures 18 and 19
for the horizontal and vertical diameters, respectively. A smooth curve
was drawn through these values in each figure.

The mathematical determination of the principal stresses is based on
the theory given by Timoshenko (reference 8) from which the following
general equations for the principal stresses at any point in a disk under
edgewise compression with point load were derived:

$$\sigma_u = a - \frac{1}{2}\left(\sigma_1 + \sigma_2 + \sqrt{\sigma_1{}^2 + 2\sigma_1\,\sigma_2\cos 2B + \sigma_2{}^2}\right) \qquad (9)$$

$$\sigma_v = a - \frac{1}{2}\left(\sigma_1 + \sigma_2 - \sqrt{\sigma_1{}^2 + 2\sigma_1\,\sigma_2\cos 2B + \sigma_2{}^2}\right) \qquad (10)$$

Factors in equations (9) and (10) are:

$$\cos 2B = \frac{\frac{1}{16} - \frac{1}{2}(x/d)^2 (2 - \cos 2A) + (x/d)^4}{\frac{1}{16} - \frac{1}{2}(x/d)^2 \cos 2A + (x/d)^4} \tag{11}$$

$$\sigma_1 = a \frac{\frac{1}{2} - \frac{x}{d} \cos A}{(x/d)^2 - \frac{x}{d} \cos A + 1/4} \tag{12}$$

$$\sigma_2 = a \frac{\frac{1}{2} + \frac{x}{d} \cos A}{(x/d)^2 + \frac{x}{d} \cos A + 1/4} \tag{13}$$

where

σ_u, σ_v principal stresses at a point

x radial distance from center of disk to point

d diameter of disk

A angle between loaded diameter and line from center of disk to point

$a = \frac{2P}{\pi d}$

P load

From equations (9) and (10) the following formulas were obtained for the principal stresses on the horizontal and vertical diameters: On the horizontal diameter with $\phi = \frac{\pi}{2}$ and $\cos \phi = 0$,

$$\sigma_u = a \left[1 - \frac{4d^4}{(d^2 + 4x^2)^2} \right] \tag{14}$$

$$\sigma_v = a \left[1 - \frac{d^2 x^2}{\left(\frac{d^2}{4} + x^2\right)^2} \right] \tag{15}$$

On the vertical diameter with $\emptyset = 0$ and $\cos \emptyset = 1$,

$$\sigma_u = a \left(1 - \frac{d}{\frac{d}{2} - x} - \frac{d}{\frac{d}{2} + x} \right) \qquad (16)$$

$$\sigma_v = a \qquad (17)$$

The numerical value of a required to express the theoretical stresses in units of fringe order was determined by the method of least squares by using the crosses on the curves in figures 18 and 19 for the horizontal and vertical diameters, respectively. This value of a was used to determine the principal stresses in units of fringe order on the diameter at 45° to the horizontal, on the horizontal diameter, and on the vertical diameter. Points were not taken at the center of the disk because the wide fringes were difficult to locate accurately; points were not taken near the edges to avoid the initial fringes (figs. 2 and 3) and the residual fringes (fig. 12).

In figure 20 the computed principal stresses in fringe-order units are shown by the curves, and the experimentally determined principal stresses in the same units are shown by the plotted points.

DISCUSSION

A comparison of the stress distribution obtained by the photoelastic method with that obtained by the mathematical theory of elasticity is of interest. Such a comparison is given in figure 20, in which curves obtained by the theory of elasticity and points obtained by the photoelastic method are compared. The fringe value, which relates the stress to the fringe order, was obtained by fitting the mathematical curves to the experimental data of figure 20(a) to 20(d) by the method of least squares as previously described. The fringe value so determined was used in drawing the curves in figure 20(e).

The data agree with the mathematical curves reasonably well in most instances. The deviations can readily be explained by an analysis of the experimental technique. Of course, it was impossible to apply true-point loads to the disk. Also the stresses near the points of application were of necessity extremely high, and the material of the model became plastic at these points. The result was the development of local areas of approximate hydrostatic stress which increased the horizontal tension in adjacent parts of the specimen. The presence of such tensile

.stresses is indicated in figure 20(a). These plastic areas also tend to decrease the vertical compressive stress at the center of the specimen and to increase it near the ends of the horizontal diameter. (See fig. 20(d).) Of course, the photoelastic method is not expected to yield accurate stresses at locations in the specimen at which plastic flow is present; thus the measured stresses at or near the residual fringes shown in figure 12 are in error. This error is shown in figure 20(c) and 20(e).

The data taken on the 45° diagonal of the disk serve best as a verification in the improved photoelastic method, since it was necessary to use the isostatic lines obtained by the stress-coat method (fig. 13) to determine the experimental values. Although the principal stresses on the vertical and horizontal diameters could have been obtained by Drucker's method, the improved method was used, with $\theta = 0$ or $\frac{\pi}{2}$, because of the simplicity of its application. On the 45° diameter, the ratio of the photoelastically observed principal tensile stress to the computed value is 1.00 at the center of the disk and 1.10 at the position 0.4 of the radius from the center. This ratio for the compressive principal stress is 0.96 at the center of the disk and 0.94 at 0.4 of the radius from the center. Stresses closer to the edge of the disk are considered to be inaccurate because of the errors previously discussed.

CONCLUDING REMARK

It can be concluded that the improved oblique method of photoelastic analysis yields reasonably accurate results over regions of the photoelastic model which are not subjected to excessive stress concentrations.

Forest Products Laboratory, Forest Service
    U. S. Department of Agriculture
        Madison, Wis., July 15, 1946

REFERENCES

1. Vose, R. W.: An Application of the Interferometer Strain Gauge in
     Photoelasticity. Jour. Appl. Mech., vol. 2, no. 3, Sept. 1935,
     p. A99.

2. Brahtz, J. H. A., and Soehrens, J. E.: Direct Optical Measurement of
     Individual Principal Stresses. Jour. Appl. Phys., vol. 10, no. 4,
     April 10, 1939, p. 242.

3. Frocht, Max M.: Isopachic Stress Patterns. Jour. Appl. Phys.,
     vol. 10, no. 4, April 10, 1939, p. 248.

4. Bubb, F. W.: The Photoelastic Interferometer. Proc., 13th Semiannual
     Eastern Photoelasticity Conference, June 12-14, 1941.

5. Drucker, D. C.: Photoelastic Separation of Principal Stresses by
     Oblique Incidence. Jour. Appl. Mech., vol. 10, no. 3, Sept. 1943,
     pp. A156-A160.

6. Frocht, M. M.: Discussion. Jour. Appl. Mech., vol. 11, no. 2,
     June 1944, pp. A125-A126.

7. Durelli, Augusto J.: Experimental Determination of the Isostatic Lines.
     Jour. Appl. Mech., vol. 9, no. 4, Dec. 1942, pp. A155-A160.

8. Timoshenko, S.: Theory of Elasticity. McGraw-Hill Book Co., Inc.,
     1934, p. 104.
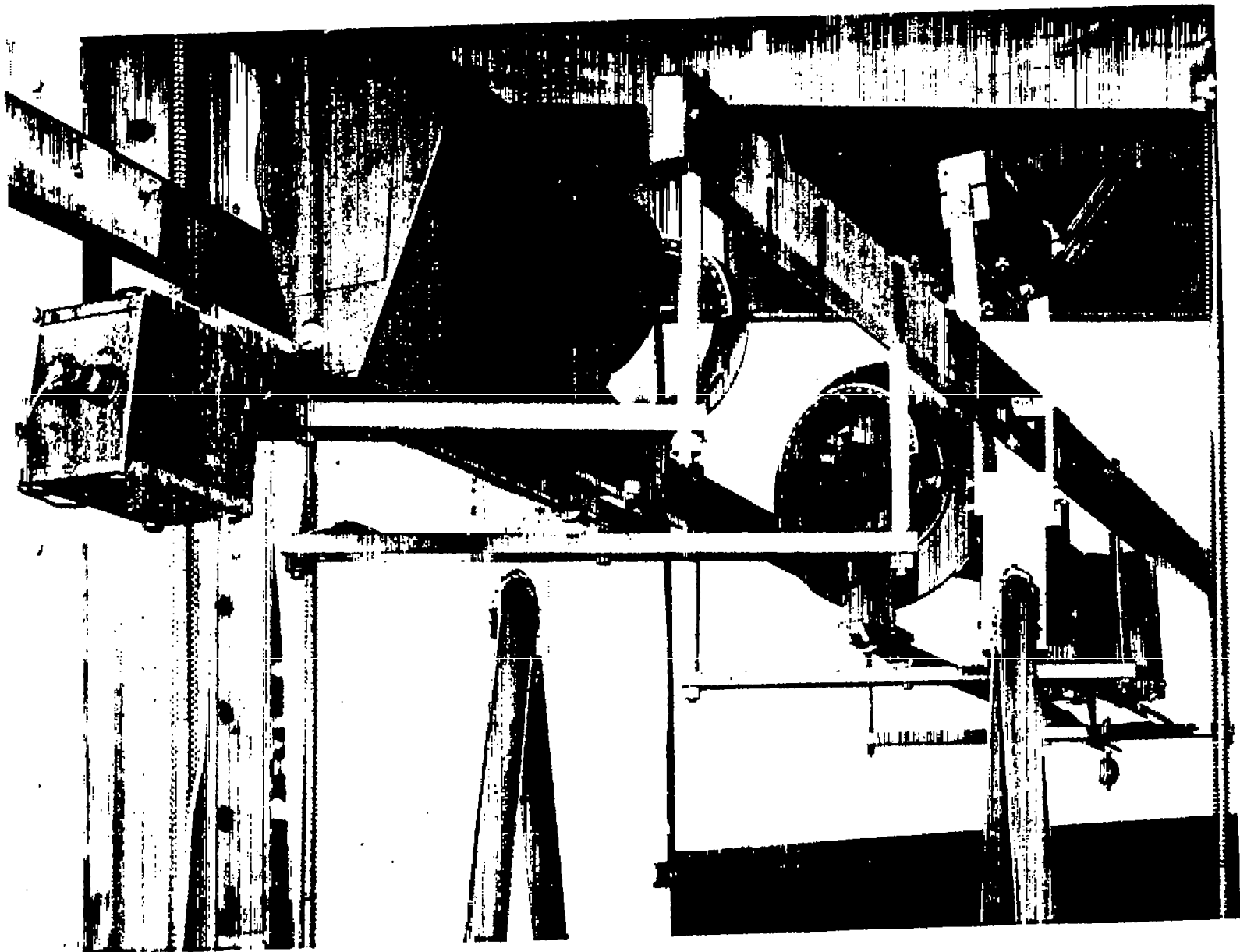
Figure 1.- Polariscope and supporting rig placed in testing machine.
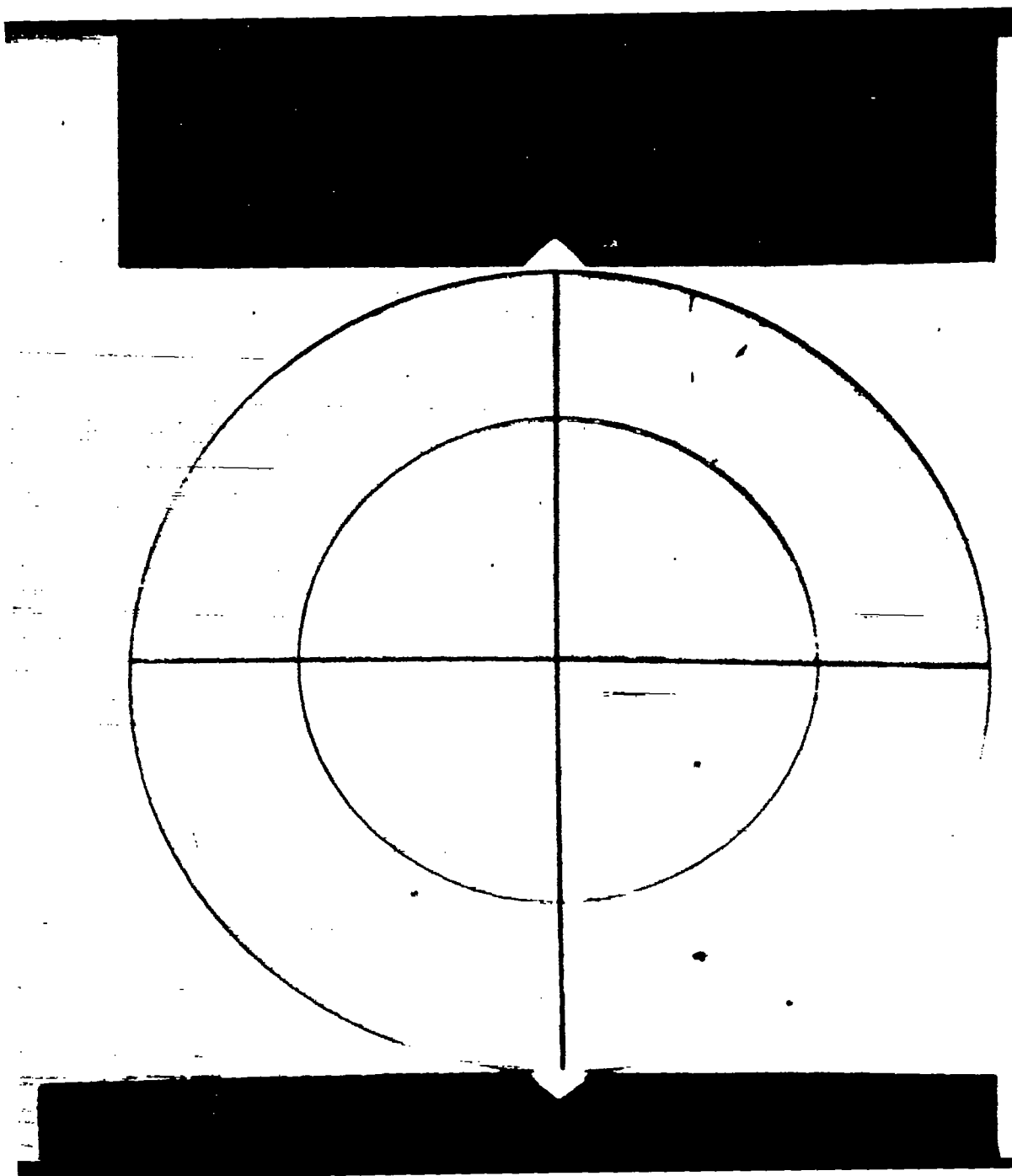
Figure 2.- Disk before load was applied. Light normal, white background.
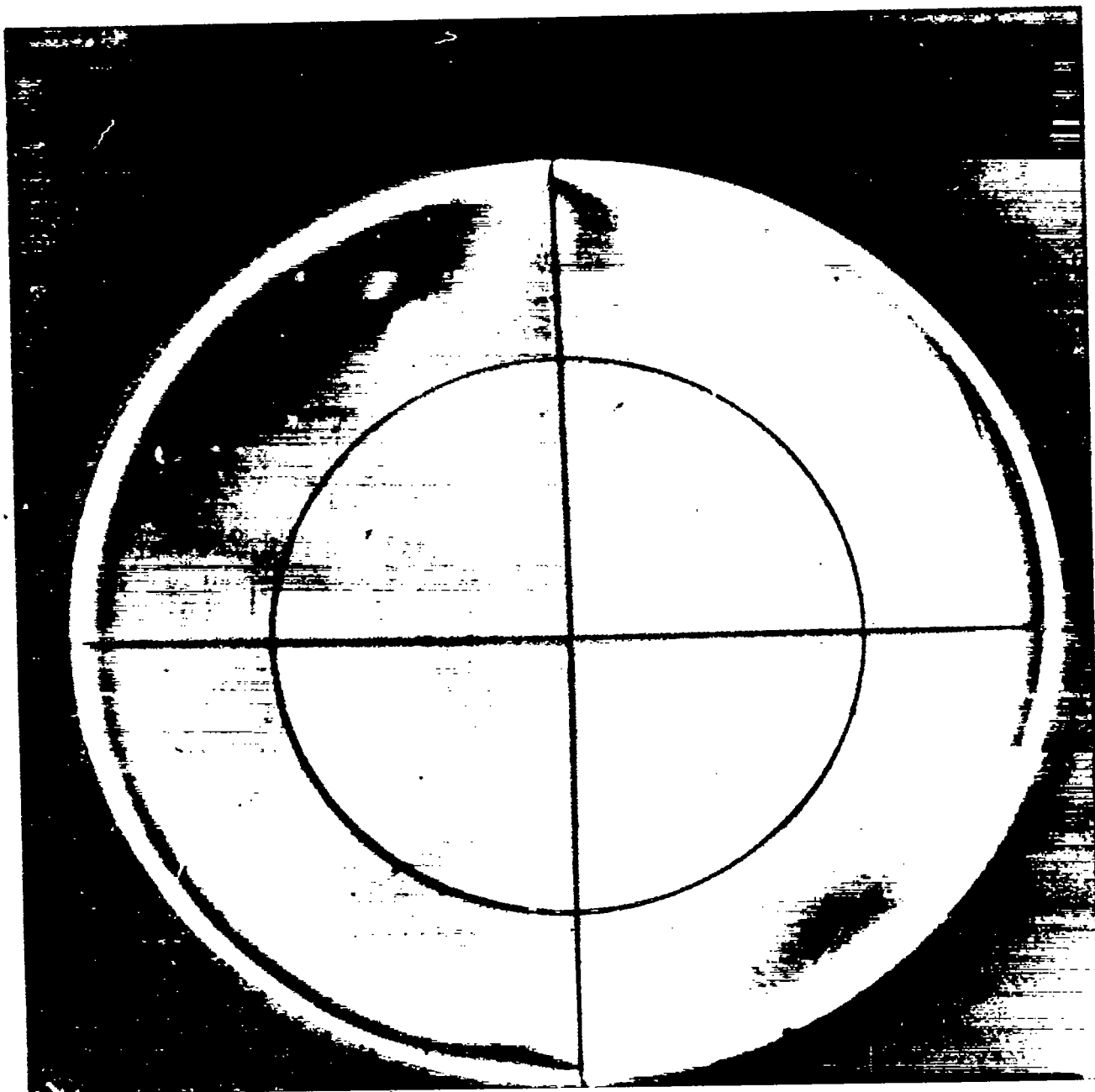
Figure 3.- Disk before load was applied. Light, normal, dark background.
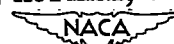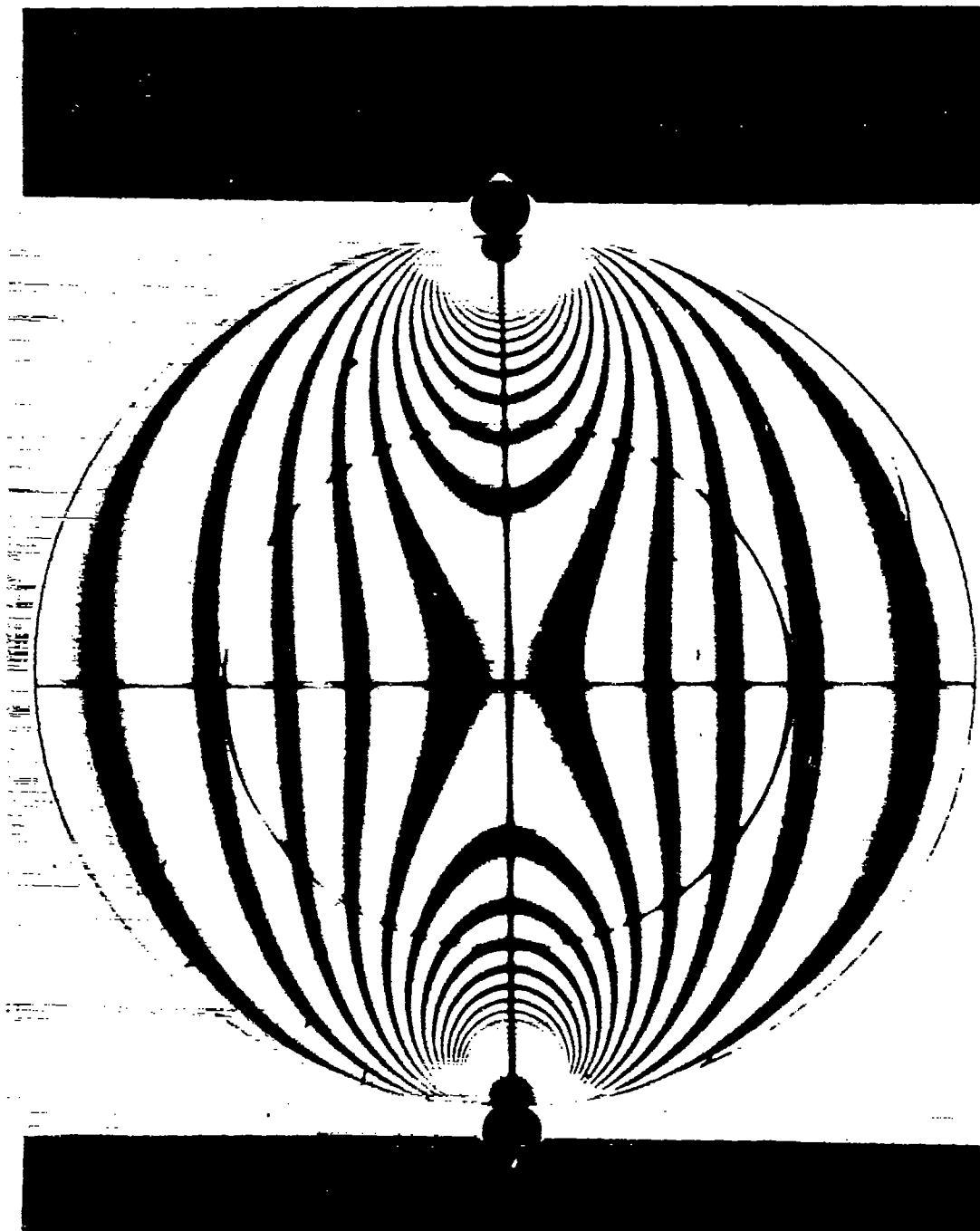
Figure 4.-   Disk under load.   Light normal, white background.
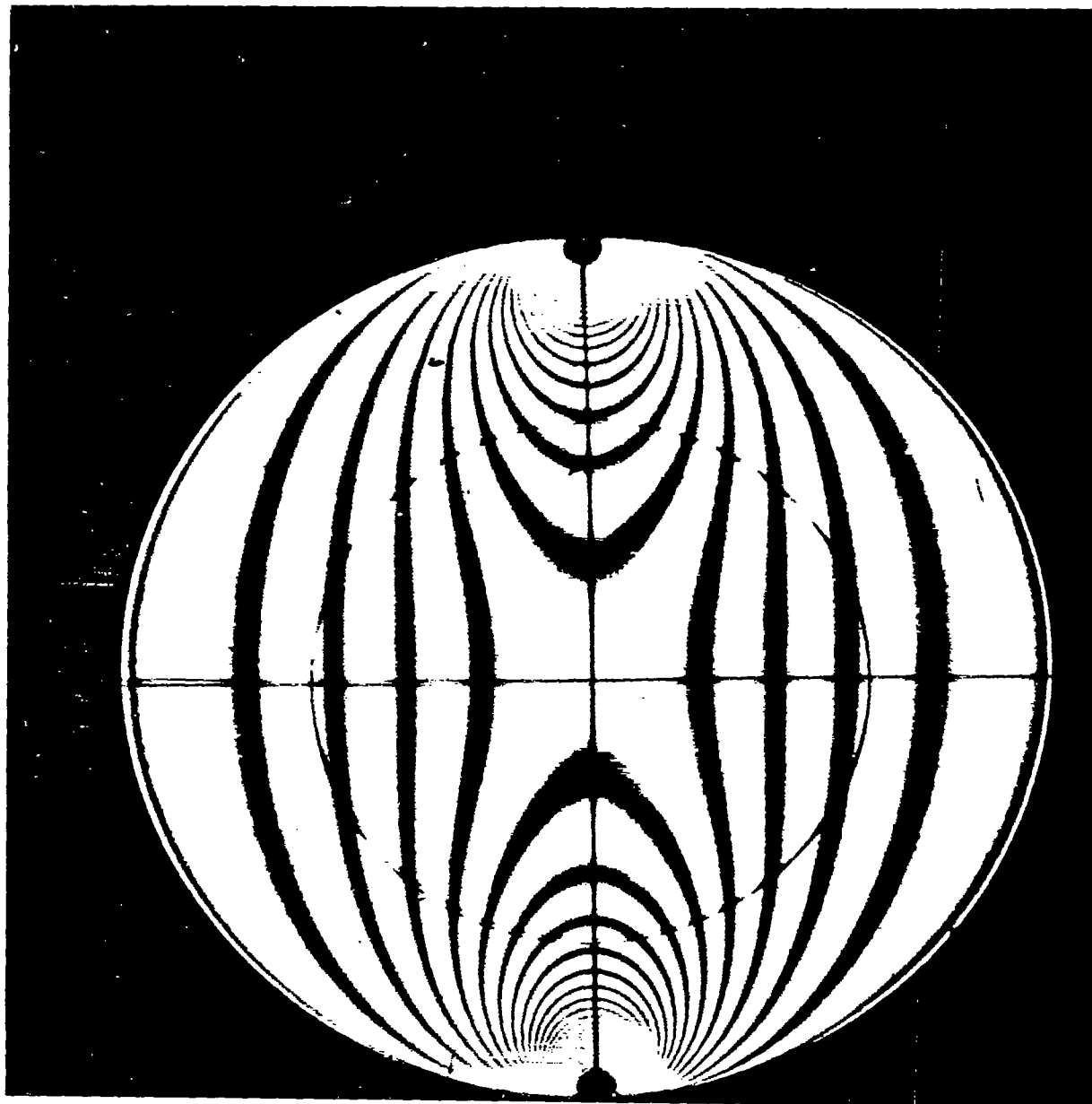
Figure 5.- Disk under load. Light normal, dark background.

Figure 6.- Disk under load. Light deflected 45°, white background.

Figure 7.- Disk under load. Light deflected 45°, dark background.
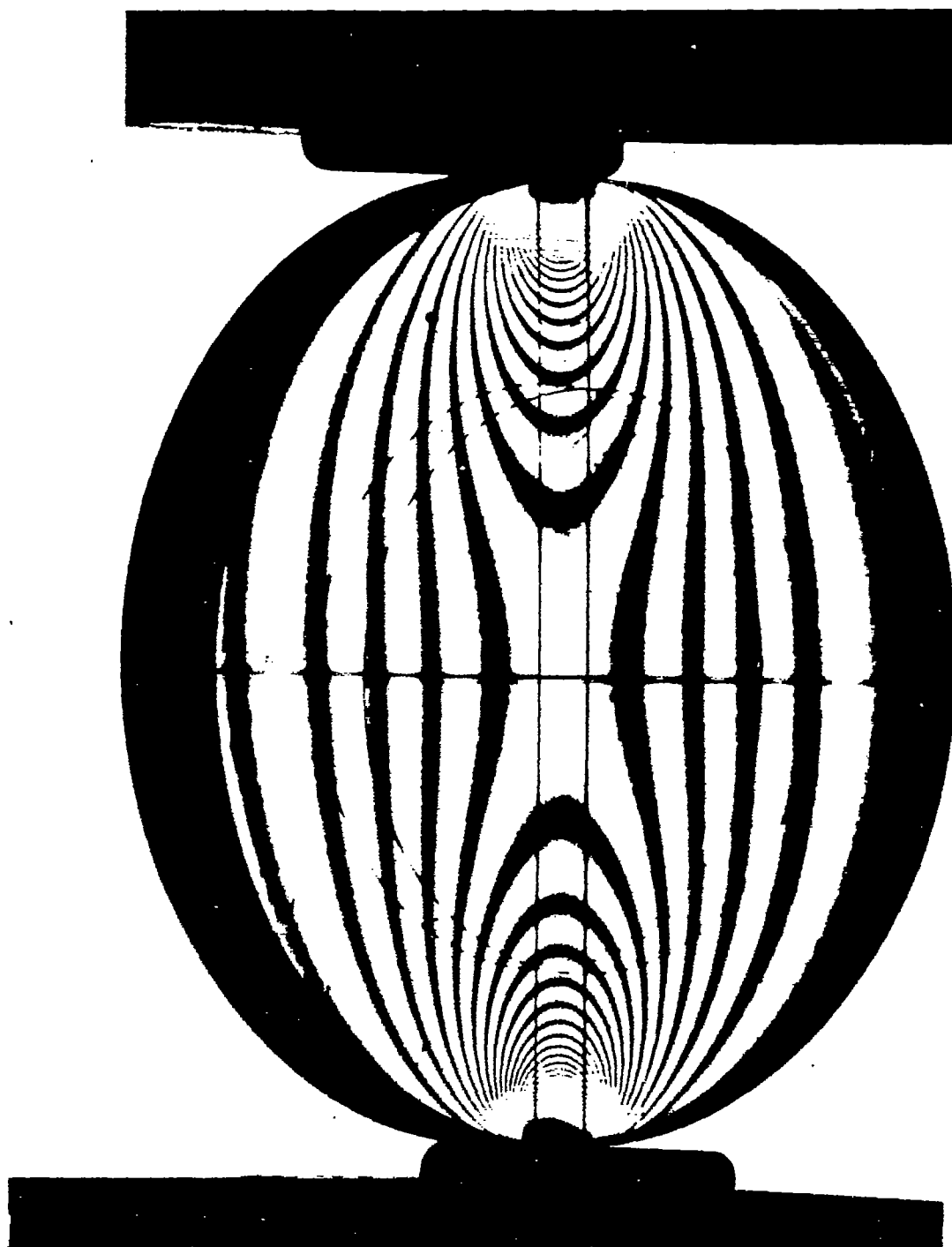
Figure 8.- Disk under load. Light rotated 45°, white background.
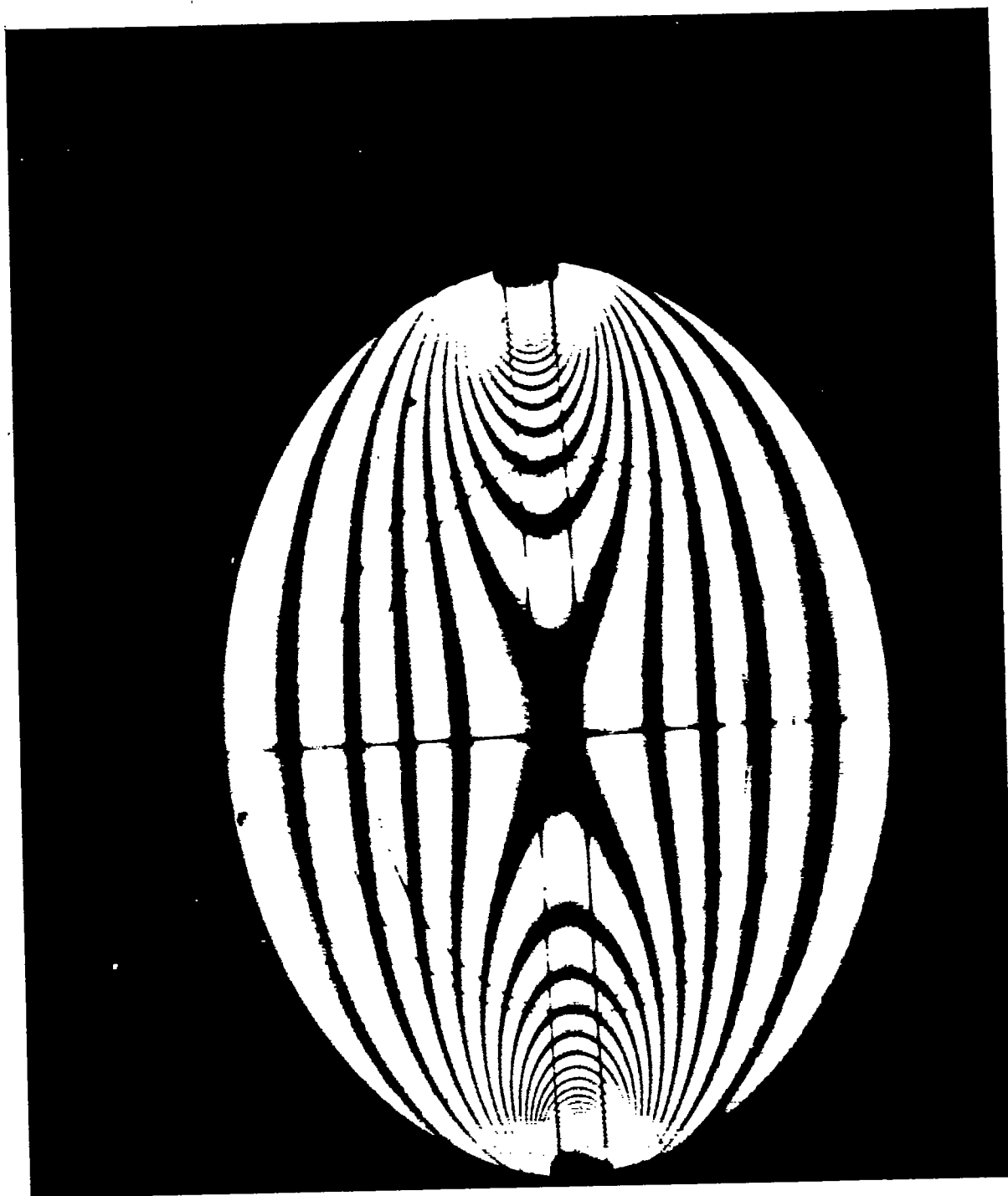
Figure 9.- Disk under load. Light rotated 45°, dark background.
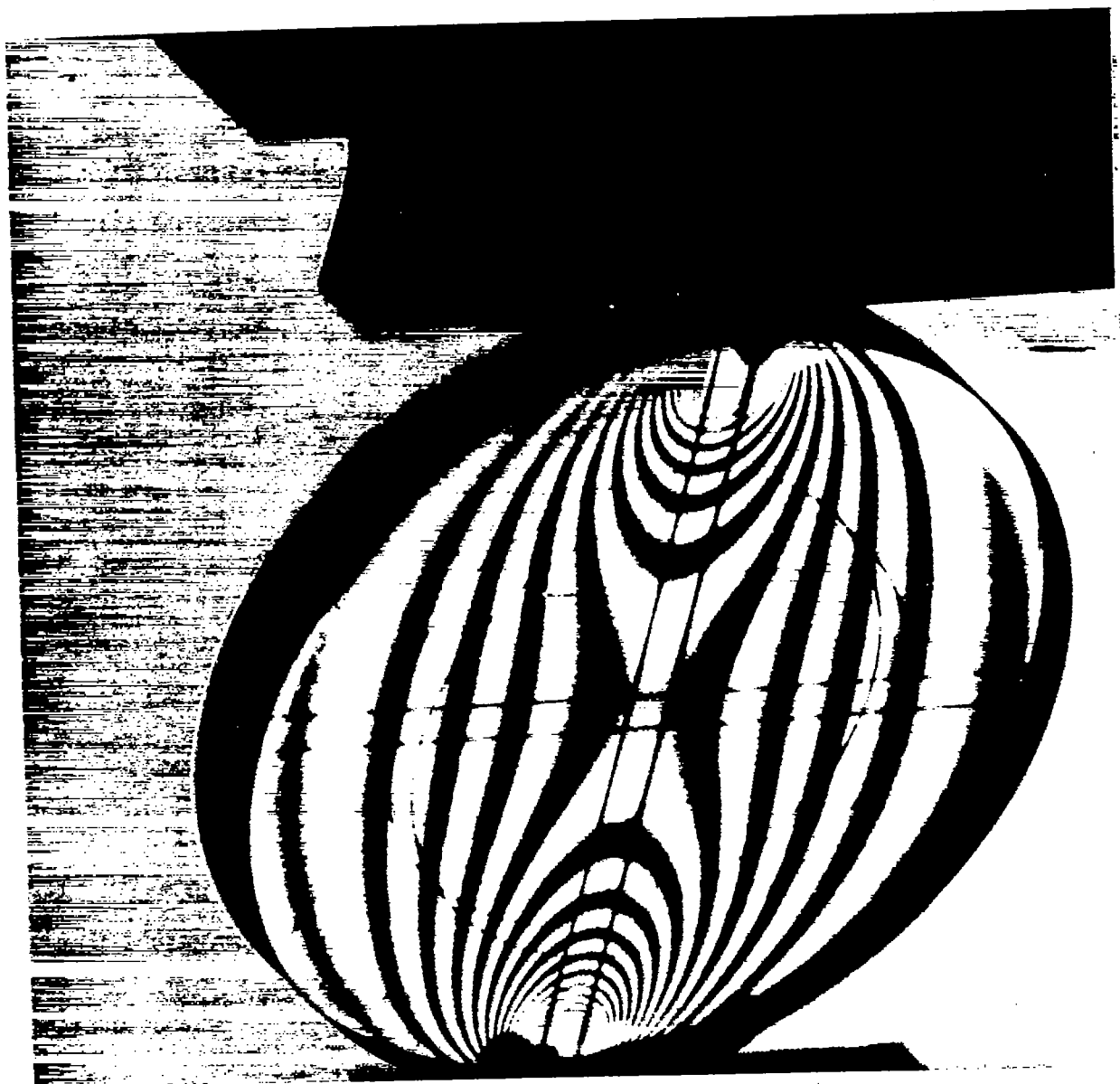
Figure 10.- Disk under load. Light oblique 48° 19', white background.
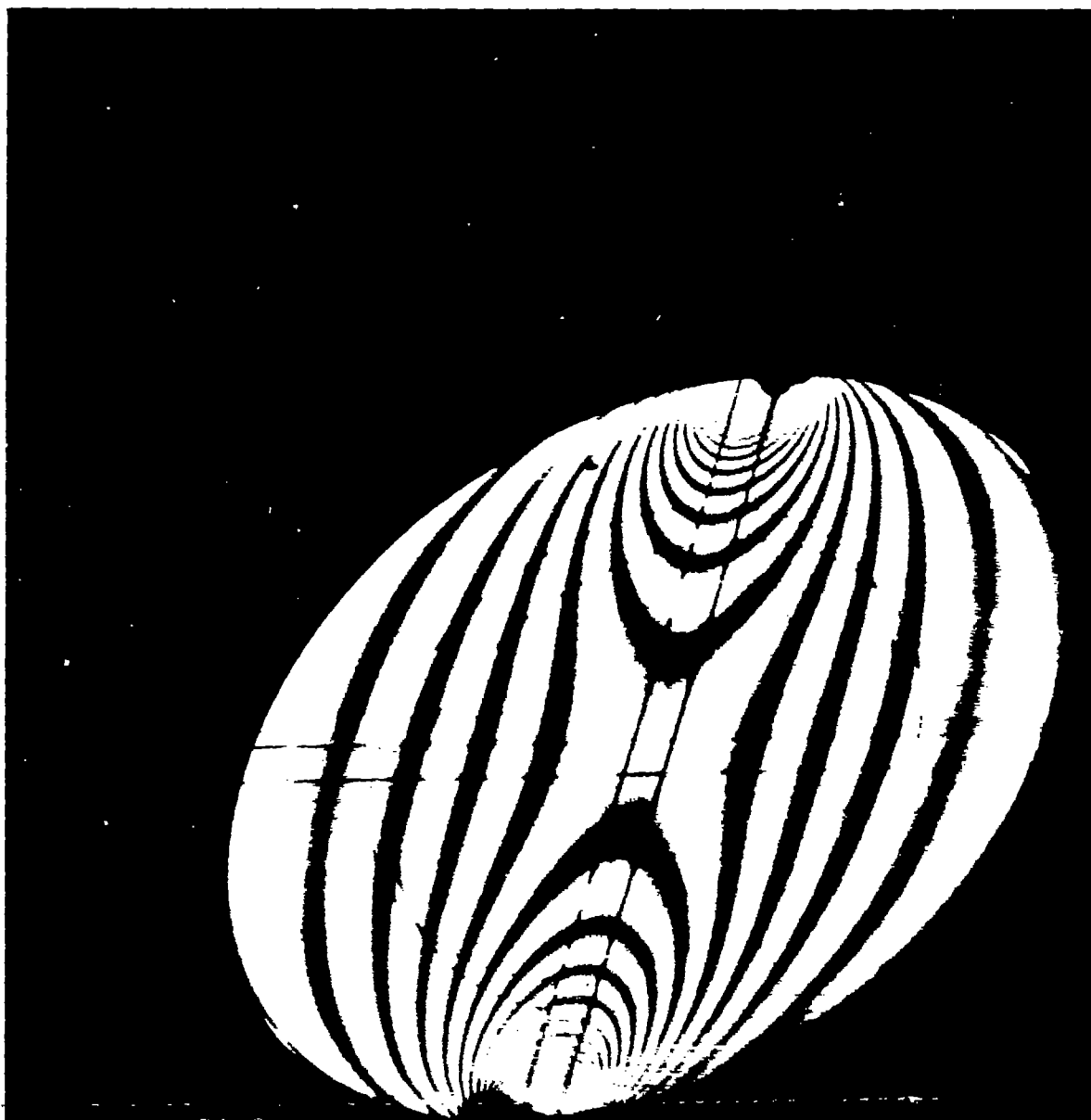
Figure 11.- Disk under load. Light oblique 48° 19', dark background.
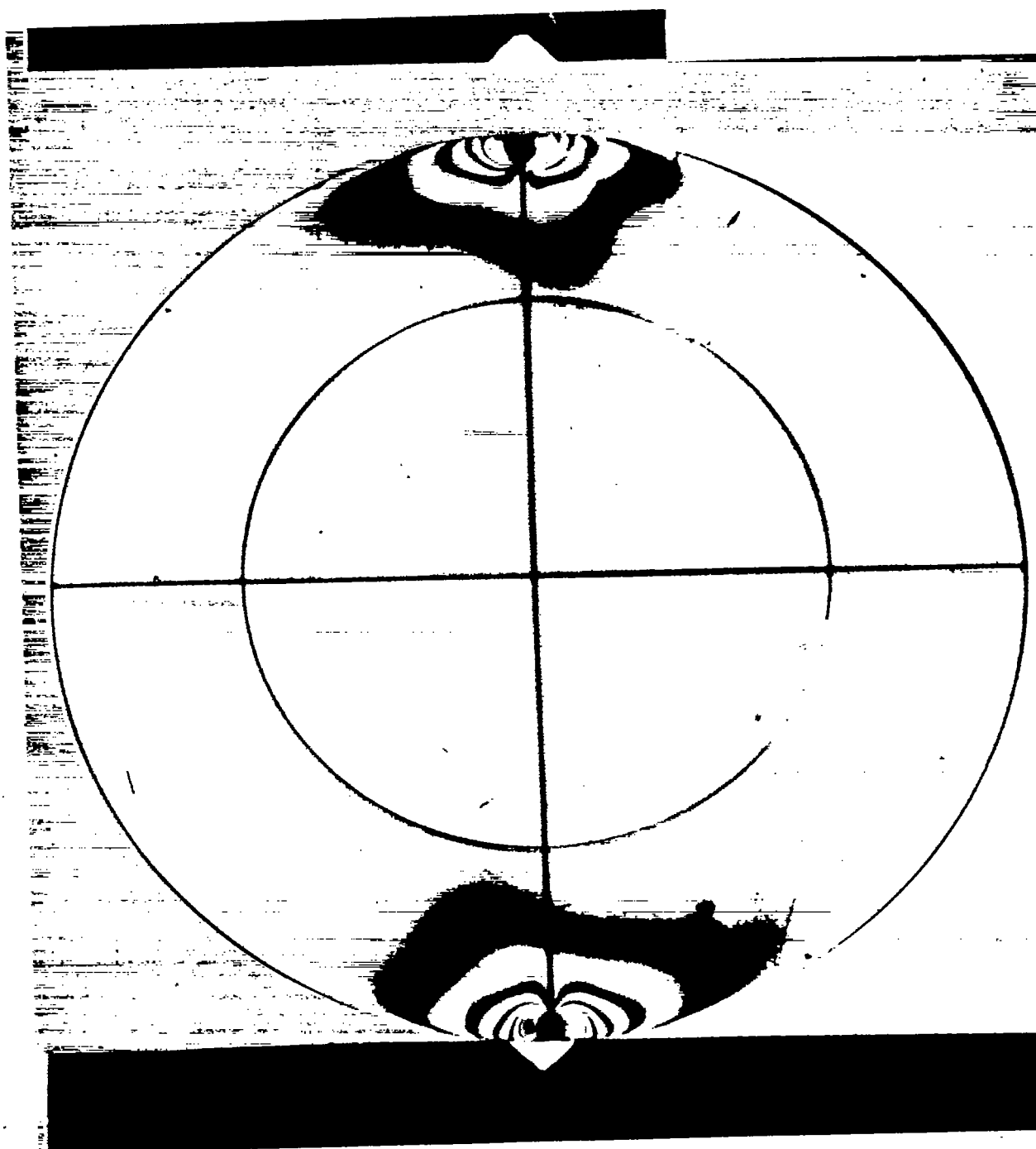
Figure 12.- Disk after load was removed. Light normal, white background.
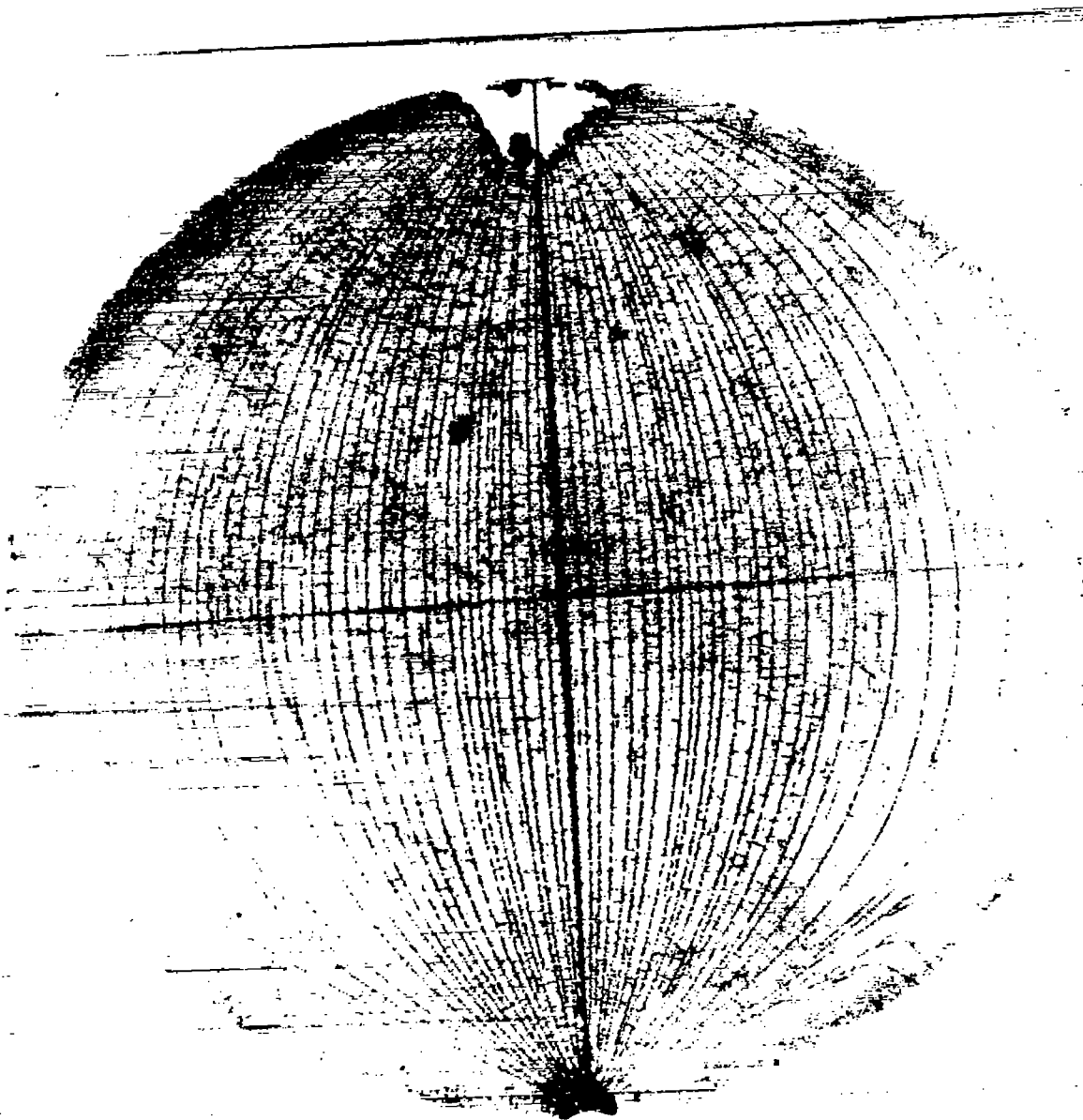
Figure 13.- Etched cracks showing directions of stress in lacquer applied to face of disk.
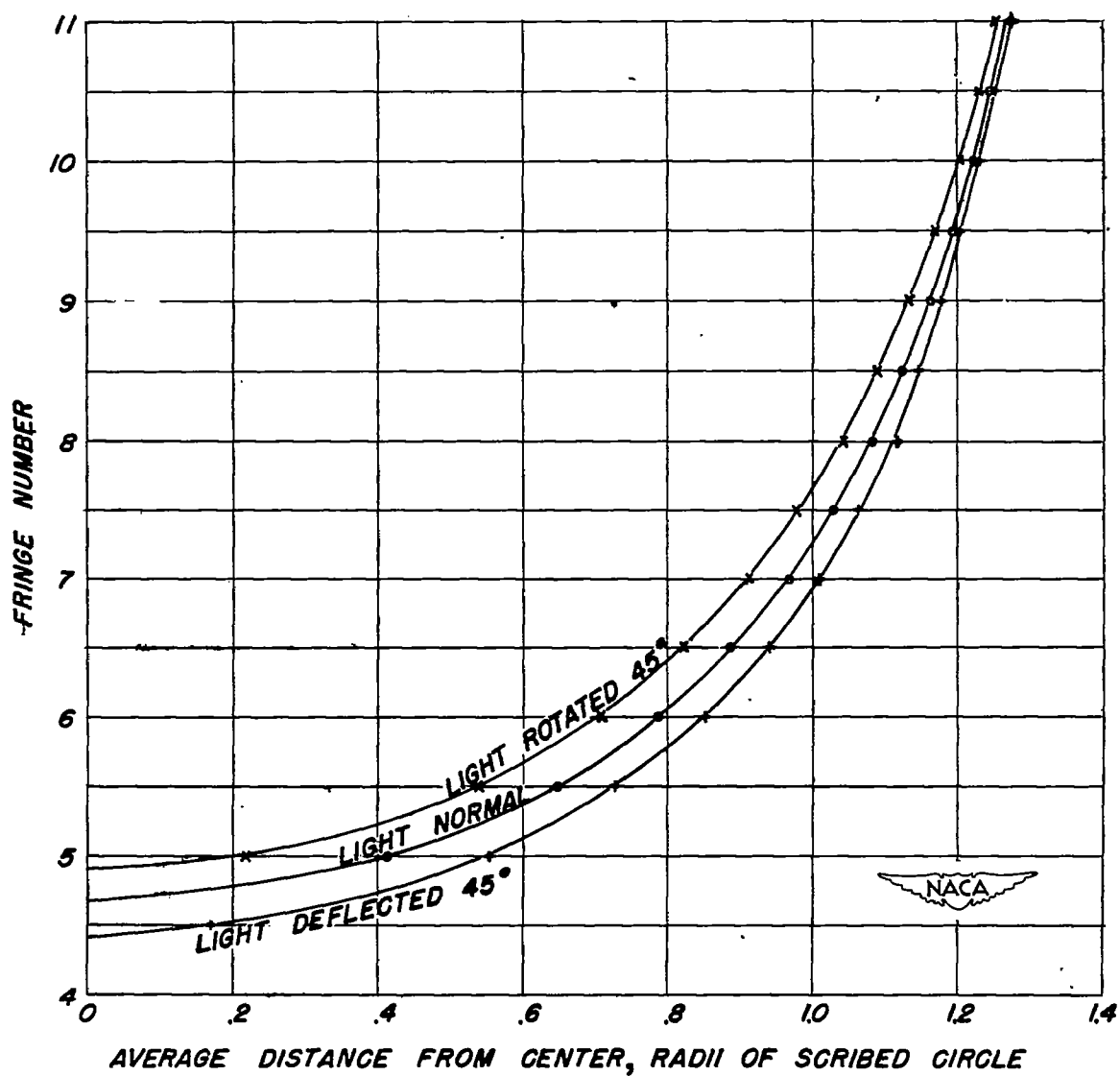
Figure 14.- Fringe-order curve for vertical diameter of disk.
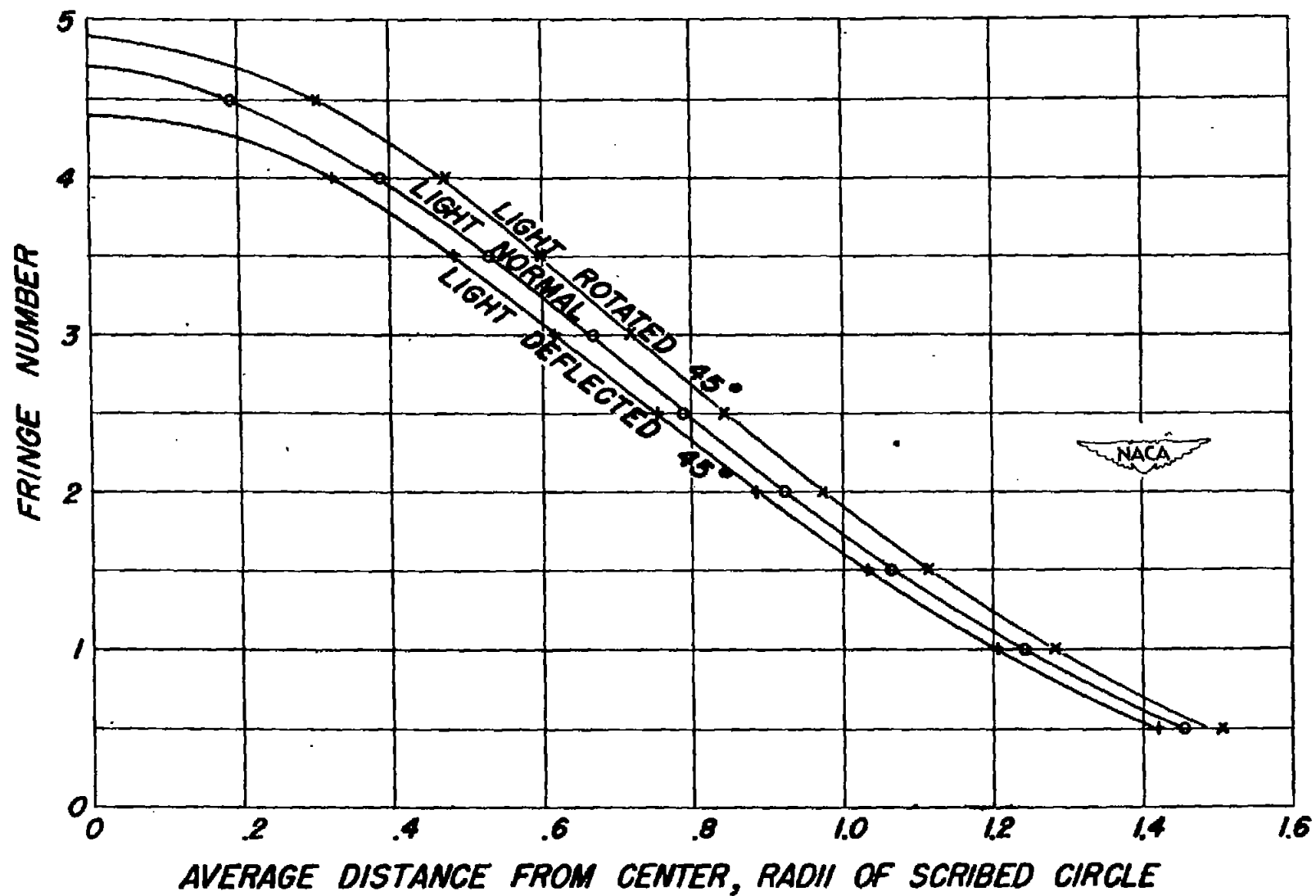
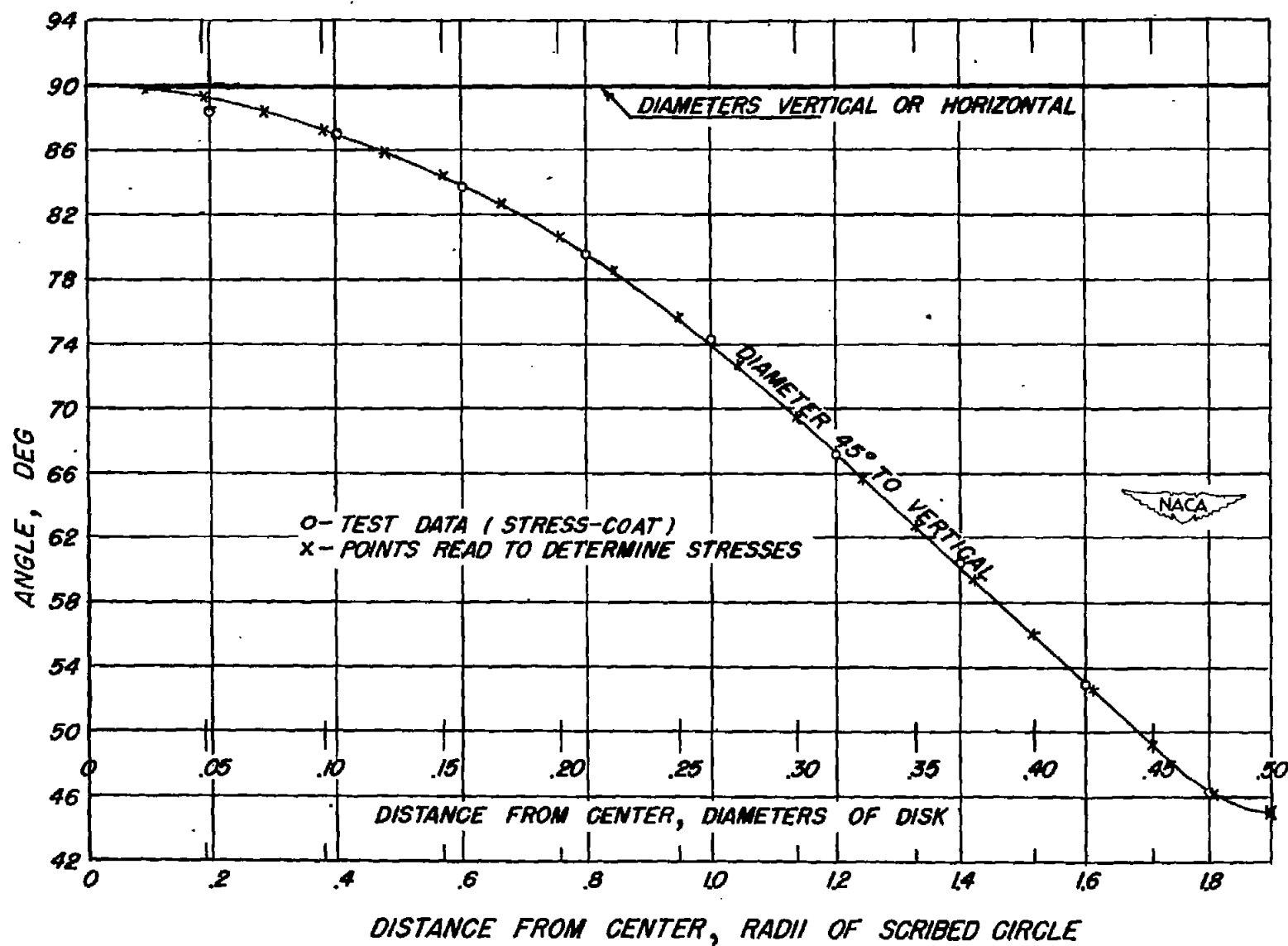Figure 15.- Fringe-order curve for horizontal diameter of disk.
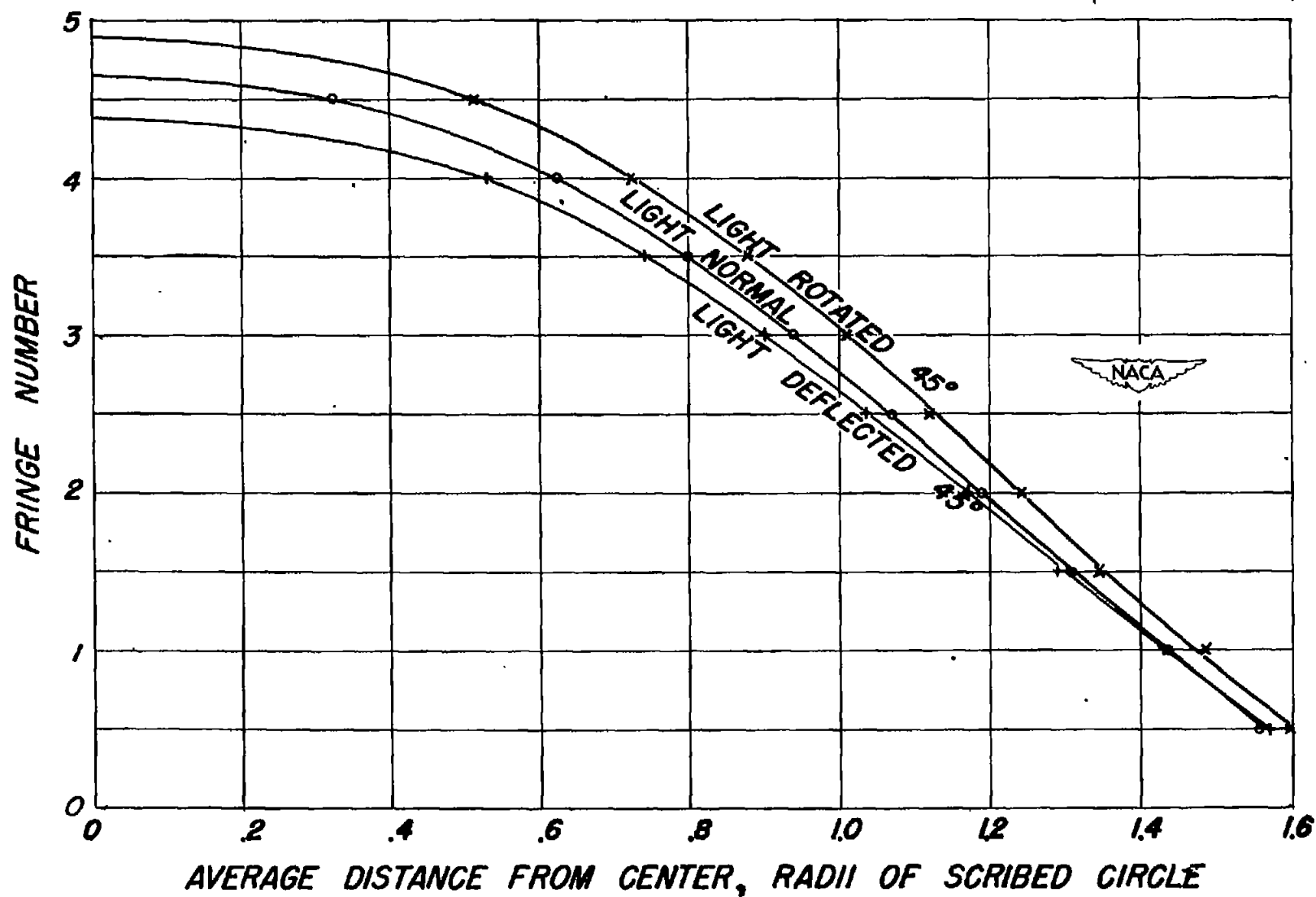
Figure 16.-· Fringe-order curve for diameter at 45° to vertical diameter of disk.

Figure 17.- Curves showing angles between principal stresses and x-axis for points on
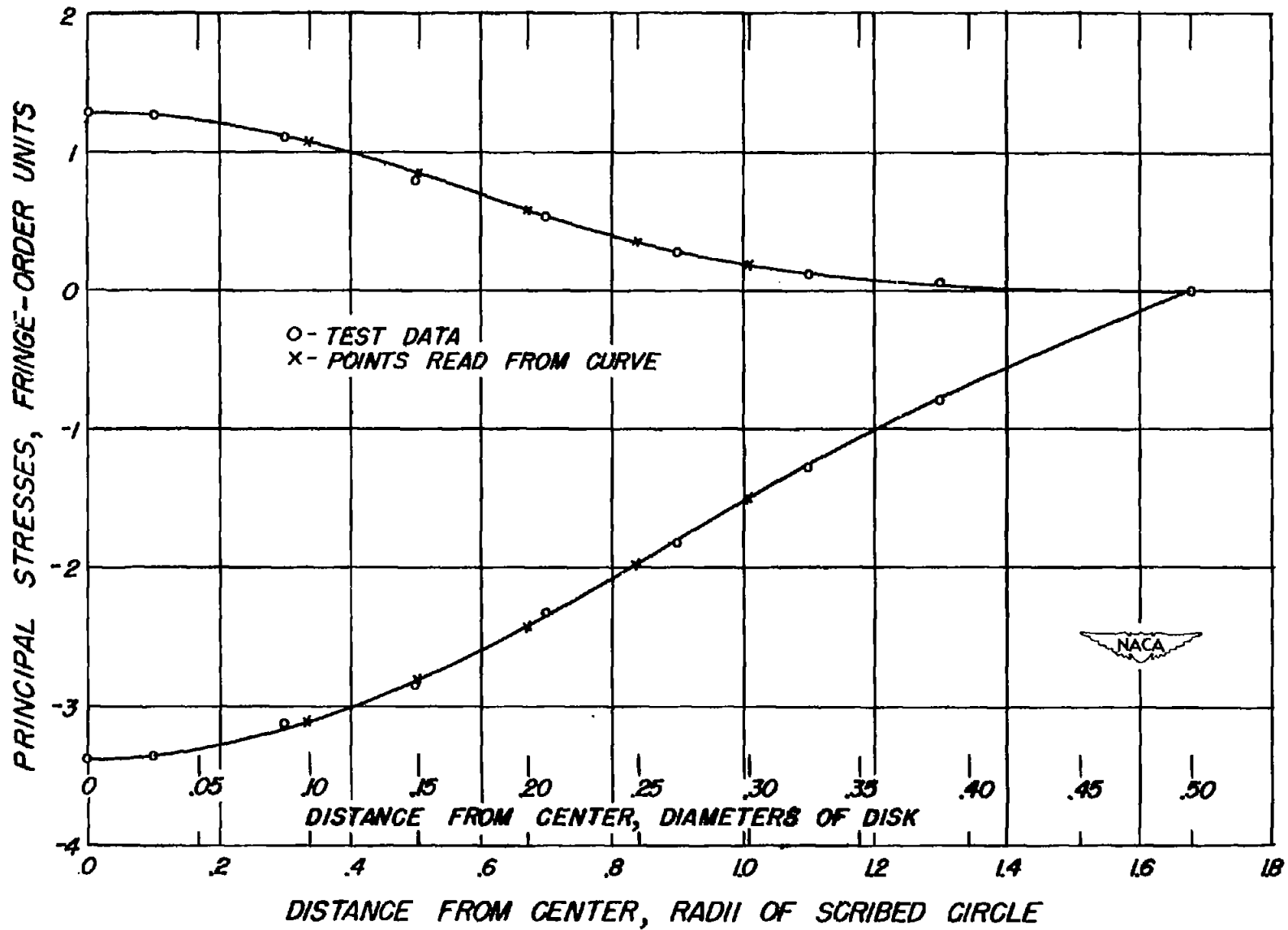horizontal, vertical, and 45° diameters.

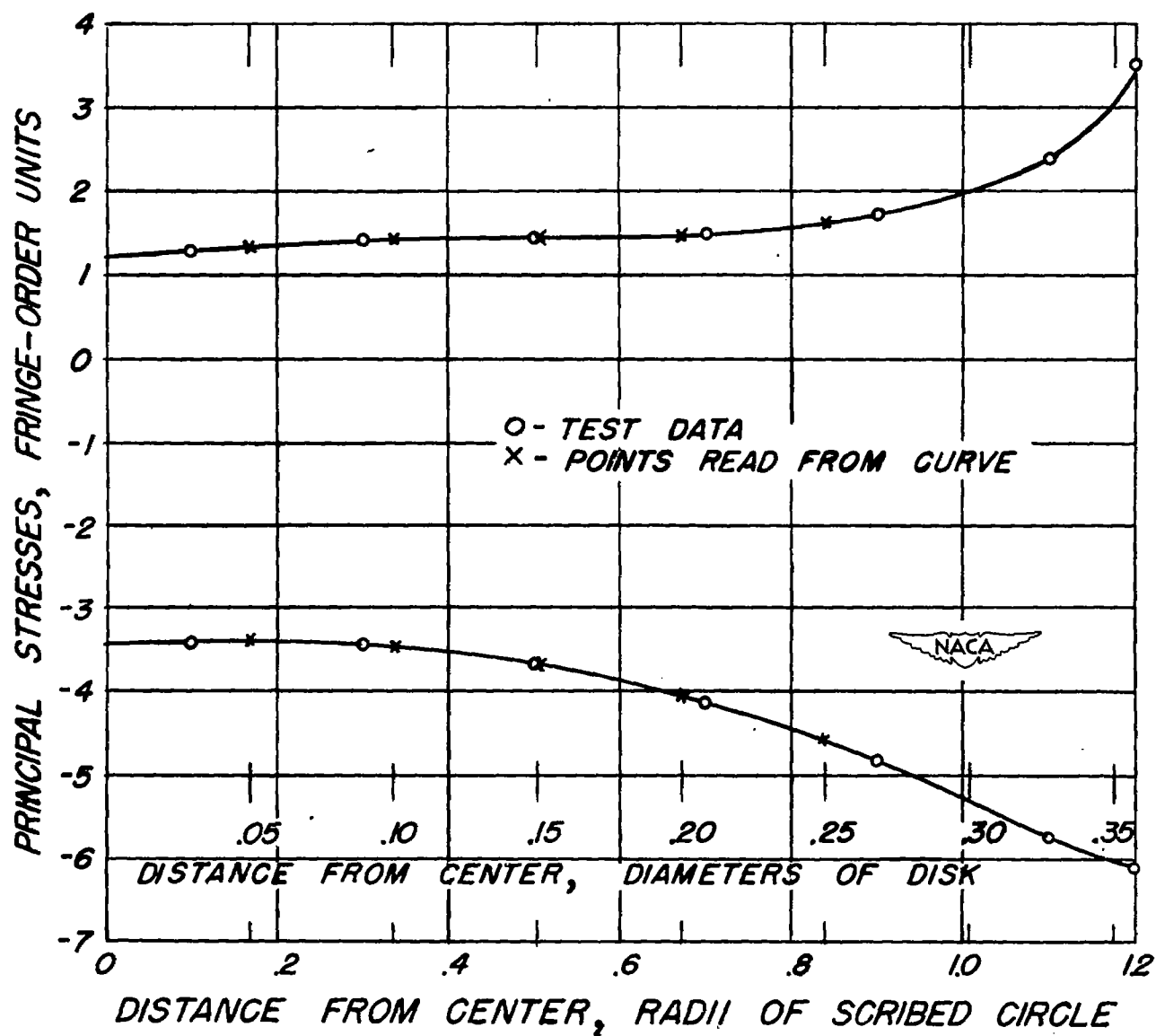Figure 18.- Principal stresses on horizontal diameter.

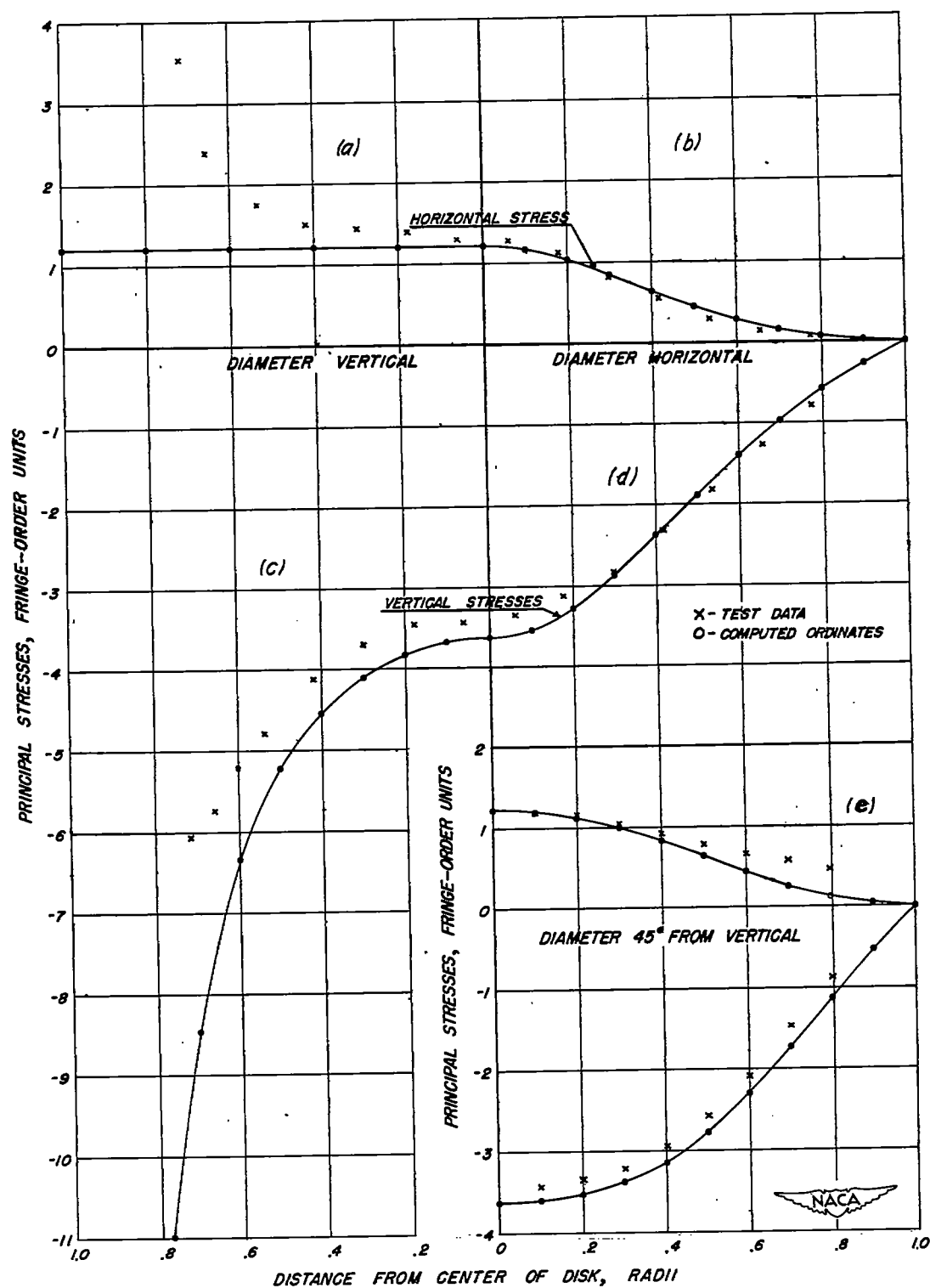Figure 19.- Principal stresses on vertical diameter.

Figure 20.- Comparison between computed and experimentally determined principal stresses.